

CERAMIC STEREOLITHOGRAPHY FOR INVESTMENT CASTING AND BIOMEDICAL APPLICATIONS

Michelle L. Griffith, Tien-Min Chu, Warren Wagner and John W. Halloran
Materials Science and Engineering Department, College of Engineering
and Biologic and Materials Sciences Department, School of Dentistry
The University of Michigan
Ann Arbor, MI

ABSTRACT

Ceramic green bodies can be created using stereolithography methods by using an ultraviolet curable suspension of ceramic powders in place of the usual resin -a "ceramic resin". We are developing ceramic resins from hydroxyapatite ceramics, to enable custom made ceramic implants by SLA, and from silica and alumina, to enable metal casting molds by SLA. We demonstrate SLA of silica, a model refractory for metal casting molds, and SLA of alumina, which present the rheological behavior and UV curing properties of several "ceramic resins", and discuss silica parts made on an SLA-250.

INTRODUCTION

Conventional StereoLithography [SLA] is used to build plastic parts from ultraviolet (UV) -curable organic resins. In the past two years, we have developed techniques to apply SLA to directly make ceramics[1,2]. Ceramic powder is dispersed in a fluid UV-curable monomer to prepare a ceramic/UV-curable monomer suspension, which we call a "ceramic resin". The building process is the same as conventional SLA. As the UV laser scans the "ceramic resin", the monomer solution is cured forming a ceramic-polymer composite layer. Layer by layer, the three-dimensional model is made from this ceramic-polymer composite to create a shaped "green" ceramic. After the building, the green ceramic object is heated in a furnace to remove polymer and sinter the final ceramic.

This paper presents progress on two ceramic SLA projects. One project [involving TMC] is concerned with the fabrication of custom-made hydroxyapatite (HA) ceramic implants. The other project [by MLG] involves fabrication of refractory ceramics. For both, the key issue is the preparation of an appropriate ceramic resin that has a viscosity low enough to use in an SLA [about 3,000 cps or less] and a curing depth sufficient for typical layer thickness [at least 200 μm].

Our long range goal for custom-made ceramic implants will build implants from CT scans, using methods developed for surgical models [3], with the implant is designed and built from hydroxyapatite by SLA. Hydroxyapatite has been used in the clinics in the bulk form for bone substitutes or as coatings for metallic implants for about 20 years[4] for its ability to form a direct contact with the regenerated bone tissue[5-7].The first step, reported here, is the development of an HA ceramic resin has the appropriate rheology and cure behavior, and which can be patterned and fired without degrading the hydroxyapatite. For refractory ceramics, our long range goal is to directly fabricate ceramic investment casting shells and cores by SLA. We report on the SLA properties of a silica resin and an alumina resin.

Ceramic resins have the same relationship between cure depth, C_d , and the energy dose, E , as conventional resins, although the mechanism of attenuation is different. Instead of adsorption, cure depth is limited by scattering of the UV radiation, since ceramic suspensions are turbid. The cure depth for ceramic suspensions can be related to the properties of the resin by:

$$[1] \quad C_d \propto \frac{\beta}{\phi} \frac{d}{\Delta n^2} \ln \left[\frac{E}{E_c} \right]$$

The penetration depth is controlled by the particle size (d), is inversely proportional to the volume fraction (ϕ) of ceramic and strongly dependent upon refractive index difference between the ceramic and the UV-curable solution, Δn . The critical energy dose, E_c , is the minimum dose required to gel the suspension. The term β involves the interparticle spacing and the UV wavelength, but is not yet well understood.

MATERIALS SYSTEMS

Ceramic Resins

The ceramic resins were made by dispersing ceramic powders in a water-based UV-curable solution consisted of acrylamide and methylene bisacrylamide monomers (2), which are similar to gel casting formulations used for molding ceramics(8). The refractive index was adjusted in the range of 1.382-1.441. The silica resin was made from powder with a broad size distribution large average particle size of 2.3 microns. The refractive index of silica is 1.56. The alumina powder was commercial sinterable powder with a average particle size of 0.34 microns. The refractive index of alumina is 1.76. The commercial hydroxyapatite powder had a submicron primary particle size, but was agglomerated into porous 10-40 micron secondary particles. The alumina and silica were dispersed in the solution at a solids loading of 50 volume percent, producing suspensions with viscosity less than 500 mPa-s [at 3 sec⁻¹], using polyelectrolyte dispersants. The HA was more difficult to disperse. Consequently its viscosity was measured as a function of pH and concentration of an anionic polyacrylate dispersant. A mixture of photoinitiators were used in the formulation: 0.4 w/o phosphine oxide and 0.7 w/o ketone derivative, which is the maximum solubility of these photoinitiators in water. These were added as the last step prior to use.

EXPERIMENTAL

The viscosity of a suspension with 20 vol% of HA powder in the monomer solution was determined with a Brookfield DV-II+ viscometer at 60 rpm. prepared. The pH value of each sample was adjusted with ammonium hydroxide in the range of from 4 to 8. An anionic surfactant (Phreeguard 1000N[%]) dispersant was added incrementally and the viscosity was measured. Isoviscosity lines were mapped at different combinations of dispersant dose and pH. With this iso-viscosity plot, the range of the pH value and the dose of the dispersant to produce the lowest viscosity of the suspension was defined.

Initial testing of the cure properties were done with a Hanovia conveyORIZED desktop UV-curing apparatus with a UV lamp[@]. The two strongest lines emitted by the lamp, 313 nm and 366 nm, correspond closely to the wavelengths used in SLA machines, 312 nm for the He-Cd laser and 351 nm for the Ar-ion laser. The exposure was determined by using a radiometer. After

[%] Calgan Corp. Pittsburgh, PA

[@] Hanovia UV Laboratory System, Hanovia, Newark, NJ

exposure, the polymerized sample was removed from the remaining uncured suspension, and the cure depth was measured by optical or electron microscopy.

Silica and alumina resin were tested in a SLA-250 machine using an Ar-ion laser. The critical exposure (E_c) and penetration depth (D_p), were determined for each suspension with the "windowpanes" test geometry(9) and fit to Equation 1. The Ar-ion laser results agreed the UV lamp data at the same energy density. Several three-dimensional parts were fabricated. The curing properties of the HA suspension were illustrated with the UV lamp apparatus, using a simple mask made in the shape of a cartoon skull.

RESULTS

I. Silica and Alumina

Equation 1 assumes that the cure depth is limited by scattering from the ceramic rather than by adsorption by the photopolymer system. It predicts that cure depth should be inversely proportional to the volume fraction ϕ of the dispersed ceramic. Figure 1 shows that this relation is indeed observed for alumina and silica suspensions in a medium with refractive index of 1.381. If scattering is the limiting factor, Eq. 1 also predicts that the cure depth should vary with $1/\Delta n^2$. This is observed in Figure 2 for a variety of silica suspensions, showing that the refractive index difference is the dominating factor controlling the depth of cure in strongly scattering systems. This is discussed in detail elsewhere (10).

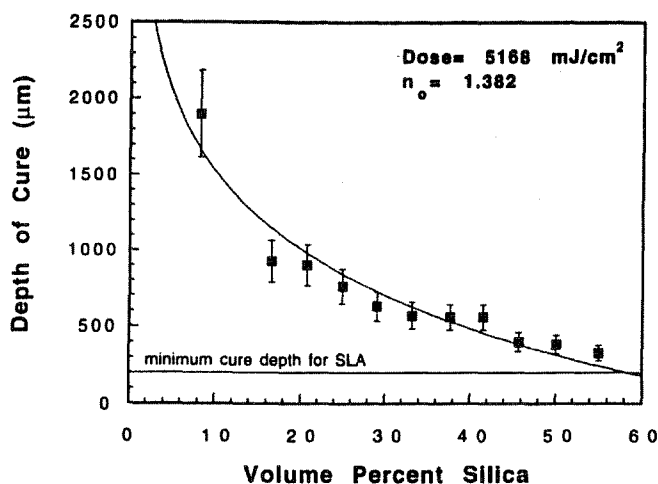


Figure 1 Cure depth vs. inverse volume fraction solids for silica and alumina dispersed in UV-curable solution

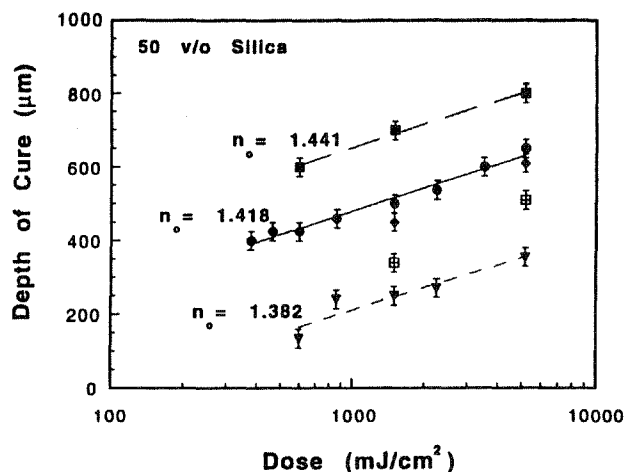


Figure 2 Cure depth vs. refractive index difference for 50 vol% silica in UV-curable solutions

Figure 3 is a photograph of the first three-dimensional ceramic green body fabricated using stereolithography. The object built is a hollow box, 1" x 1" x 0.75", with a 45 degree angle on one side. This was fabricated from 50 v/o silica dispersed in the aqueous solution having a refractive index of 1.418. The SLA parameters used were $D_p = 150 \mu\text{m}$ and $E_c = 80 \text{ mJ/cm}^2$. There are 136 layers, each 150 μm thick. The build time for this hollow box was about 4 hours. The sides and the 45 degree angle are built quite accurately. There was no problem with interlayer adhesion. The top of the box is slightly rounded because the recoat blade was not used because the sample was built in an experimental mini-vat. Instead the z-wait time was extended to 45 seconds

to allow the new layer to equilibrate to a reasonably flat surface. The bottom of the box is warped, due to curling of the first layers, probably because of the raster-style build style and inadequate support structure. In spite of the imperfections in this first attempt, we consider this a demonstration of practical ceramic SLA. The silica box was heated to 1000°C to simulate the firing cycle of ceramic molds.

Figure 4 shows the microstructure of an alumina part fabricated on the SLA-250 and subsequently sintered at 1550 °C. This appears to be a high quality dense alumina ceramic, typical of pore-free fine grained alumina ceramics. This demonstrates that SLA-fabricated ceramic green bodies can sinter as readily as conventional ceramics. This is discussed elsewhere (11).

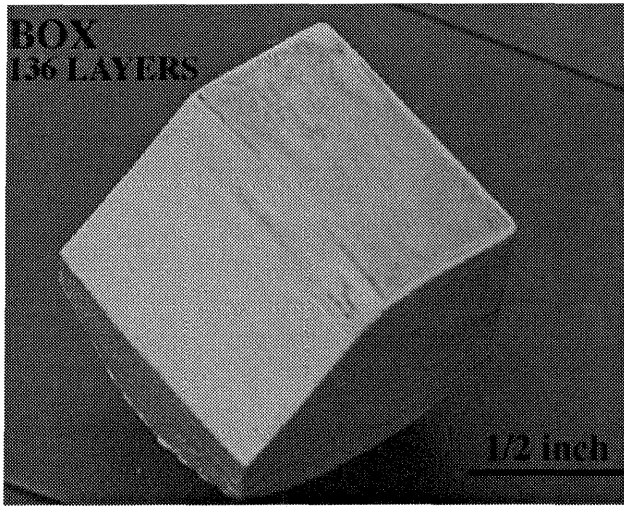


Figure 3 Hollow "box" part fabricated on SLA-250 from silica ceramic resin

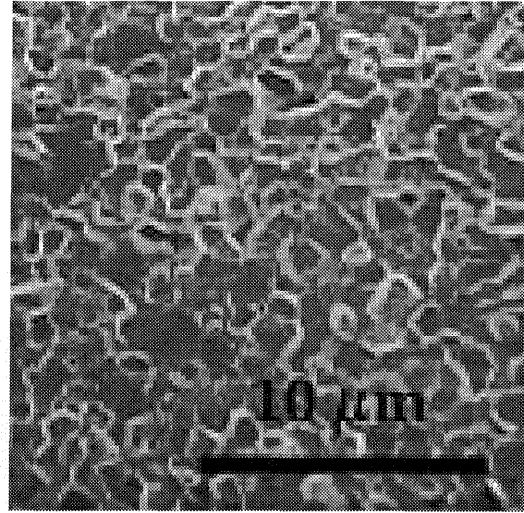
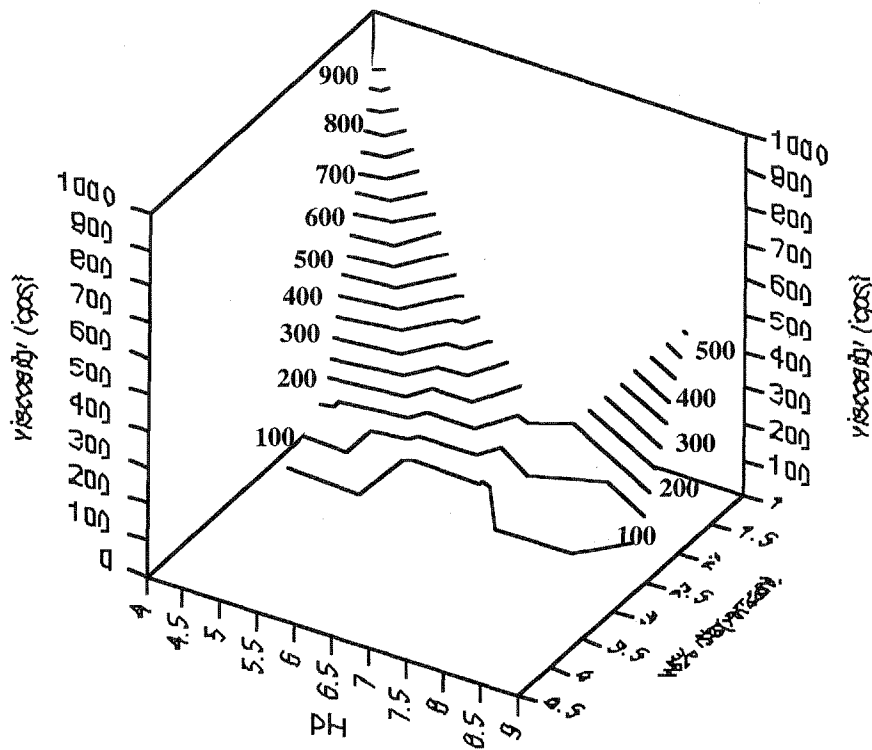


Figure 4 SEM micrograph of the fracture surface of alumina fabricated on SLA-250 sintered 1550°C for 2 hr, showing fine-grained pore-free microstructure

II. Hydroxyapatite

The viscosity of the dispersion of HA powder in acrylamide solution depends upon pH and the amount of polyacrylate dispersant. A 20 vol% HA-AM/MBAM suspension with 1.46 wt% dispersant equilibrates after mixing to a pH of 6.48. At a constant dispersant dose, viscosity is a minimum around pH 7. Higher dose of dispersant reduces the viscosity over the whole pH range, resulting in a wider low-viscosity region at higher dose of dispersants. Figure 5 shows this behavior as an iso-viscosity plot. After the dose of the dispersant exceeded 2.5 wt% of the dry powder, the viscosity of the suspension in the whole pH range dropped under 100 cps. To establish the effect of HA content, the solids-loading of the suspension was increased from 10 vol% to 45 vol% at a dispersant dose of 3 wt% of dry powder and pH 7, as shown in Figure 6. The viscosity of the suspension increased from 10 cps to 2960 cps. The viscosity of the suspension rose rapidly to above 12,000 cps when the vol% ceramic was increased from 45 vol% to 46.5 vol%.



20 Vol% HA in AM/MBAM

Fig.5 Iso-viscosity contours vs. pH and dispersant dose for 20 vol% HA in AM/MBAM

Cure Depth and Pattern Reproduction

The 45 vol% HA suspension had a cure depth of 280 μm , which is adequate for SLA. The linear relation of cure depth vs. $1/\phi$ is also obeyed for HA powders, as shown in Figure 7. From this we predict that a cure depth larger than 200 μm will be achievable up to 55 vol%. Figure 8 is a demonstration of the pattern reproduction with the HA ceramic resin. On the left is the skull cartoon "mask", made from xeroxed transparency, with the HA /polyacryamide green ceramic layer on the right. The change in the dimension was due to the scattering of the light at the edge of the crude xeroxed mask since the light source we used was not a point light source. This should not happen when we use a laser on the SLA-250 machine.

Green Body Property Characterization

The hydroxapatite does not appear to be degraded by this process. Figure 9 is the x-ray diffraction pattern of the hydroxyapatite green body after making the HA ceramic resin, curing, and binder burnout. Only HA is present, which indicates that the hydroxyapatite structure was preserved during the whole process.

CONCLUSIONS

Highly concentrated suspensions of ceramic powders in photopolymerizable solutions can be cured by UV lamps or UV laser. Cure depth is proportional to the logarithm of energy through a Beer-Lambert relation, with the depth of penetration limited by scattering of UV radiation. Depth

of penetration is inversely proportional to ceramic volume fraction and to the square of the refractive index difference between the ceramic and the suspension medium. Multilayer parts have been built using a SLA-250 with an Ar-ion laser, with promising accurate parts with good interlayer adhesion. These first ceramic objects demonstrate the feasibility of stereolithography for directly building green ceramic objects, both for sintered structural ceramic parts and for refractory ceramic shells and cores for metal casting.

The cure depth of a 45 vol% HA suspension was 280 μm , which is above the minimum depth requirement. The hydroxyapatite structure in the green body was retained after polymer binder burnout.

ACKNOWLEDGMENT

This research on refractory ceramics is supported by the Office of Naval Research under grants N00014-93-1-0302 and -95-1-0527, through Dr. S. Fishman and R. Wachter. The biomedical research is supported the the University of Michigan through a Rackham Grant to T-M-Chu. We thank Paul Jacobs, Thomas Pang, and Kelle Kwo of 3D Systems for their help.

REFERENCES

1. M.L. Griffith and J. W. Halloran, *Proceedings of the SFF Symposium*, University of Texas at Austin Publishers, Austin, 1994, pp. 396-403.
2. Michelle L. Griffith, Ph.D. thesis, The University of Michigan, Materials Science and Engineering Department, March 1995.
3. N.G. Stoker, N.J. Mankovich, and D. Valentino, "Stereolithographic Models for Surgical Planning: Preliminary Report," *Journal of Oral and Maxillofacial Surgery*, **50**, 466-471, (1992).
4. L.L. Hench,, "Medical and Scientific Products," In *Engineered Materials Handbook*, Vol. 4, (eds.) J. Samuel J Schneider, The Materials Information Society, 1991, pp. 1007-1013.
5. G. de Lange "The Bone-Hydroxyapatite Interface," In *Handbook of Bioactive Ceramics*, Vol. II, (eds.) T. Yamamuro, L. L. Hench and J. Wilson, CRC Press, Inc., Boca Raton, FL, 1990, pp. 61-75.
6. M. EL Deeb and R. Holmes, "Tissue Response to Facial Contour Augmentation With Dense and Porous Hydroxyapatite in Rhesus Monkey," *Journal of Oral and Maxillofacial Surgery*, **47**, 1282-1289, (1989).
7. C.A. van Blitterswijk, J.J. Grote, W. Kuijpers, W. T. Daems, and K. de Groot, "Macropore tissue ingrowth: a quantitative and qualitative study on hydroxyapatite ceramic," *Biomaterials*, **7**, 137-143, (1986).
- 8) A.C. Young, O.O. Omatete, M.A. Janney, and P.A. Menchofer,, 1991, " Gel Casting- A New Ceramic Forming Process", *Journal of the American Ceramic Society*, vol. 74, no. 3, pp. 612-618.
- 9) P.F. Jacobs, *Rapid Prototyping and Manufacturing: Fundamentals of Stereolithography*, Soc. of Manufacturing Engineers, Dearborn, p. 263-281 (1992)
- 10) M.L. Griffith and J. W. Halloran, "Photopolymerization of Turbid Suspensions", submitted to *Journal of Applied Physics*
- 11) M.L. Griffith and J. W. Halloran, "Free Form Fabrication of Ceramics by Stereolithography", submitted to *Journal of the American Ceramic Soc.*

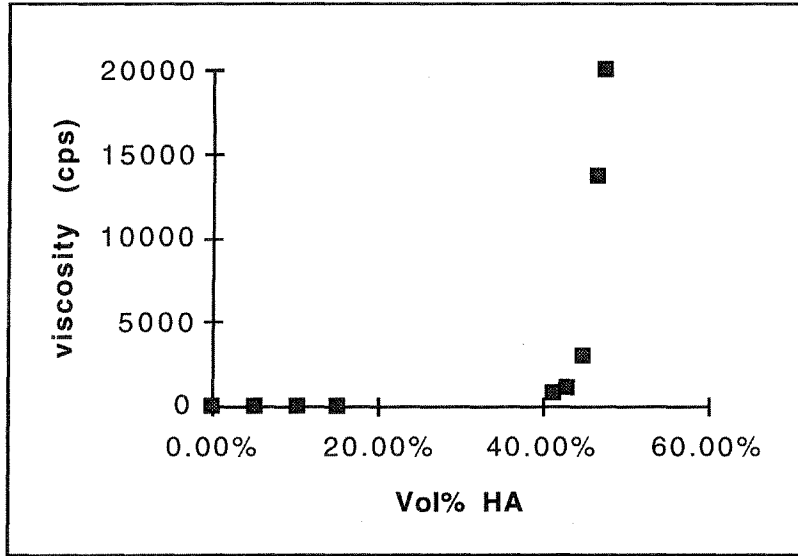


Fig. 2 Viscosity vs. vol% HA with 3 wt% dispersant

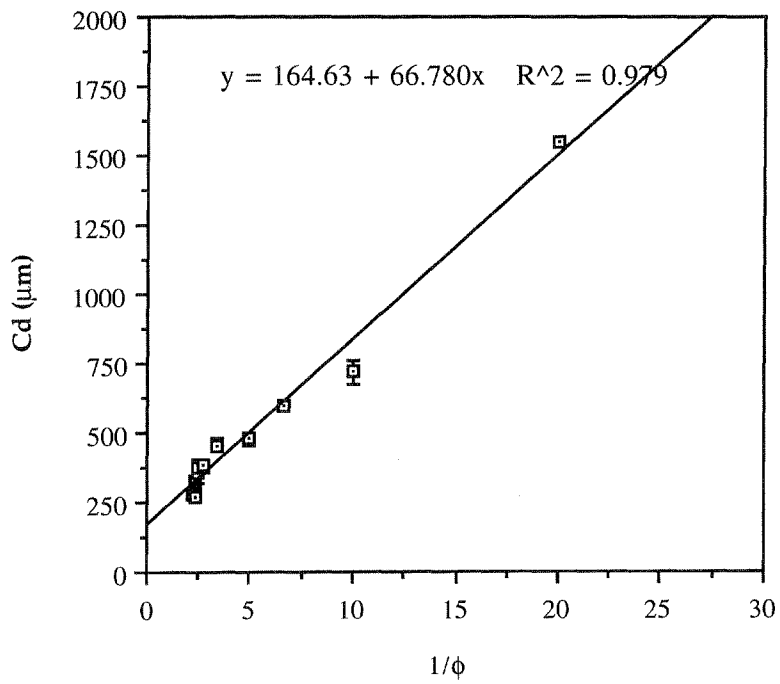


Fig. 7 Cure Depth (μm) vs. 1/φ

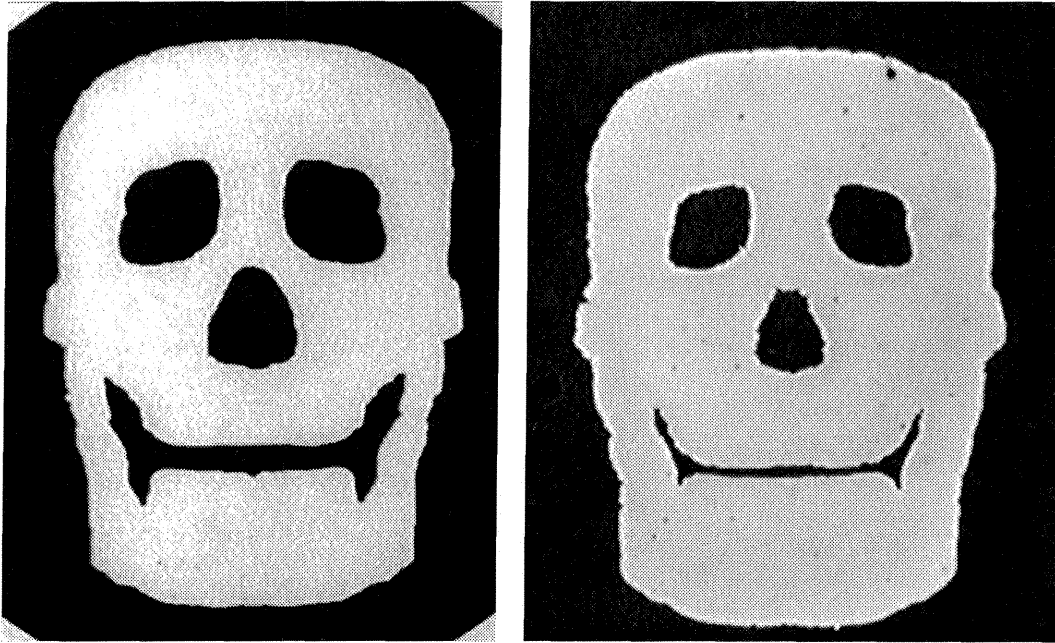


Fig. 8 The test mask (left) and the cured HA/polymer composite layer (right)

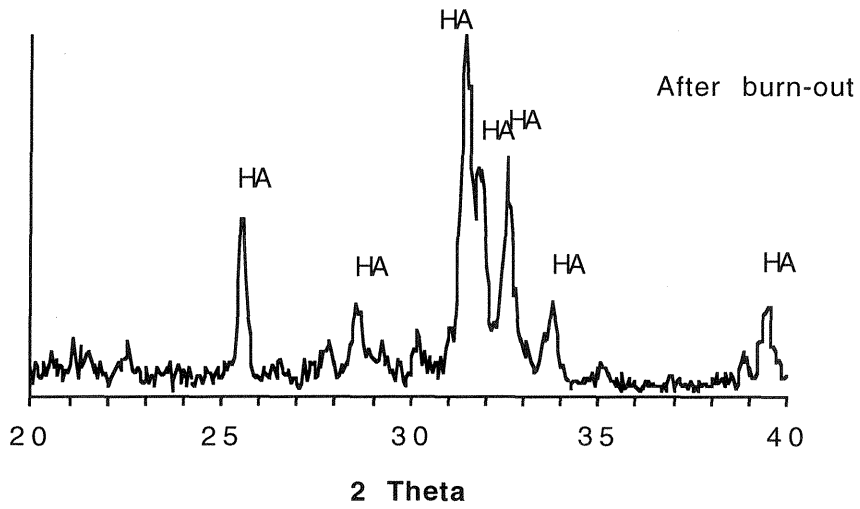


Fig. 9 X-ray diffraction pattern of final hydroxyapatite specimen after polymer binder burn-out